THE ASTROPHYSICAL JOURNAL, 306:629–641, 1986 July 15

DA WHITE DWARF EFFECTIVE TEMPERATURES DETERMINED FROM *IUE* LYMAN-ALPHA PROFILES

J. B. HOLBERG[1]
Lunar and Planetary Laboratory, University of Arizona
F. WESEMAEL[1]
Département de Physique and Observatoire du mont Mégantic, Université de Montréal
AND
J. BASILE
Lunar and Planetary Laboratory, University of Arizona
Received 1985 November 27; accepted 1986 January 3

ABSTRACT

The Lyman-α profiles of 12 DA white dwarfs have been obtained with the *International Ultraviolet Explorer Satellite*. Analysis of these profiles provides an improved, uniform, and relatively bias-free measure of effective temperature for these stars over the range 20,000–60,000 K. Simultaneous estimates of surface gravity yield a mean gravity of $\log g = 7.96$ for the entire sample, with the hottest stars tending to have the lowest gravities. A significant exception to this trend occurs in the case of the gravitation of HZ 43. An important by-product of this work has been the determination of a correction to *IUE* fluxes over the 1150–1350 Å range.

Subject headings: spectrophotometry — stars: atmospheres — stars: white dwarfs — ultraviolet: spectra

I. INTRODUCTION

The observed temperature range of DA white dwarfs extends from the vicinity of 5,000 K to possibly as high as 60,000 K, for the hottest such stars. For the bulk of the DA population, whose temperatures are well below ~30,000 K, ground-based colors provide an adequate measure of temperature. Temperature uncertainties however, increase dramatically for the hotter DAs. Extending the wavelength baseline into the ultraviolet, although helpful in some instances, often provides only a marginal gain due to uncertainties regarding the absolute fluxes at the shortest wavelengths.

A better defined temperature scale for the hot luminous end of the DA sequence would benefit several important areas of investigation. For example, since observed DA temperatures are primarily the result of a cooling sequence, it is the hottest such stars which are most recently descended from the poorly understood pre–white dwarf stages of stellar evolution. Unfortunately the temperatures, luminosities and relative numbers of these stars remain very imprecisely known. Observational comparisons with theoretical DA cooling sequences and definitions of the DA luminosity function at the high temperature end are currently limited (Fleming, Liebert, and Green 1986) by the increasing uncertainty in temperature and gravity encountered for the relatively small number of hot DAs. It is also for higher temperature DAs that significant departures from standard zero temperature mass-radius relationships, due to either finite temperature effects (e.g., Winget, Lamb, and Van Horn 1986) or to residual nuclear burning in the envelope (Iben and Tutukov 1984; Koester and Schonberner 1985), are expected.

The discovery of narrow interstellar-like features due to C, N, and Si ions in the UV spectra of hot DA white dwarfs (Bruhweiler and Kondo 1981, 1983) has led to new consideration of such processes as diffusion, radiative support of heavy ions, and the possibility of mass loss and stellar winds in these high-gravity stars. These sharp narrow features occur in most, but not all, DAs with temperatures in excess of 20,000 K and appear to be photospheric in origin, although in several of the hotter DAs evidence of a circumstellar or wind origin is strong. Questions such as the origin and location of the absorbing material within the stellar atmosphere, and the abundances of C, N, and Si ions (e.g., Wesemael, Henry, and Shipman 1984) can only be answered with detailed stellar atmosphere models including reliable effective temperatures.

Another area where knowledge of temperature is important is the issue of helium abundances in the atmospheres of hot DAs. Soft X-ray (Kahn *et al.* 1984; Petre, Shipman, and Canizares 1986) and extreme UV (EUV) observations (Malina, Bowyer, and Basri 1982) both require the presence of some short wavelength opacity source, presumably helium at abundances in excess of 1×10^{-5} hydrogen, in order to model the observed high energy fluxes from hot DA white dwarfs. At these wavelengths the observed flux of a DA white dwarf is a strong function of both temperature and helium abundance (Wesemael, Liebert, and Green 1984). In the absence of detailed soft X-ray or EUV spectra, therefore, one means of breaking the strong correlation which exists between temperature and helium abundances is to rely on accurate independent estimates of effective temperature.

Finally, DA white dwarfs, because of their relatively simple and well-determined UV energy distributions, are attractive candidates for evaluating the internal consistency and perhaps even the absolute flux scale of the *IUE* photometric calibration. The most ambitious approach to this problem is that of Finley, Basri, and Bowyer (1984) who used a sample of DA white dwarfs to determine wavelength-dependent and time-dependent modifications to the *IUE* calibration. In arriving at their result, they employed optical estimates of DA temperatures as the starting point for the generation of a set of self-consistent UV energy distributions. As we shall see, having a homogeneous set of DA temperatures is an effective way to reduce uncertainties and ambiguities in this type of work.

[1] Guest Observer with the *International Ultraviolet Explorer Satellite*.

In this paper we analyze the H I Lyman-α (Lyα) profiles of a sample of hot DA white dwarfs covering a broad range of temperatures. One of the primary goals of this study is to establish a uniform and self-consistent temperature scale, which at the low end can be linked to measurements determined from ground-based colors. The stars included in this investigation were therefore chosen to cover a range in effective temperature from ~15,000 K to the hottest DAs. Additional considerations involved previous observational history and brightness. In Figure 1 we illustrate the development of the Lyα profile as a function of temperature for eight of the stars in our sample. The analysis techniques employed here follow very closely those presented in a recent detailed study of one of our stars, CD −38°10980 (Holberg *et al.* 1985). This star is also included here since it occupies a critical part of the temperature range under consideration and demonstrates an important aspect of our treatment of the *IUE* fluxes.

II. OBSERVATIONS

The majority of the *IUE* observations discussed here were obtained as part of a program designed to secure high quality Lyα profiles for a sample of hot DA white dwarfs covering a wide range of temperatures. These observations were in turn supplemented by archival *IUE* spectra obtained from the National Space Science Data Center. All SWP spectra, their apertures, effective exposure times, and the observers who acquired them are listed in Table 1, along with the Villanova catalog white dwarf number (McCook and Sion 1984).

a) Lyman-α Profiles

For each star in our sample the Lyα profile is derived primarily from an SWP small-aperture spectrum. The advantages of this procedure have been previously discussed by Holberg and Wesemael (1984) and Holberg *et al.* (1985). The primary advantage is the nearly complete elimination of the geocoronal emission component, which is especially important for the narrower profiles characteristic of hotter DAs. Typically doubly exposed large- and small-aperture exposures were obtained and the small aperture fluxes scaled to those of the large. In several cases, principally due to overexposed red wings, the data would not support this simple procedure and composite profiles were constructed. In these instances we indicate the spectra used to construct such composites. For each star careful comparisons were made with existing, well-exposed, archival data in an effort to ensure the internal consistency of the *IUE* profile data used.

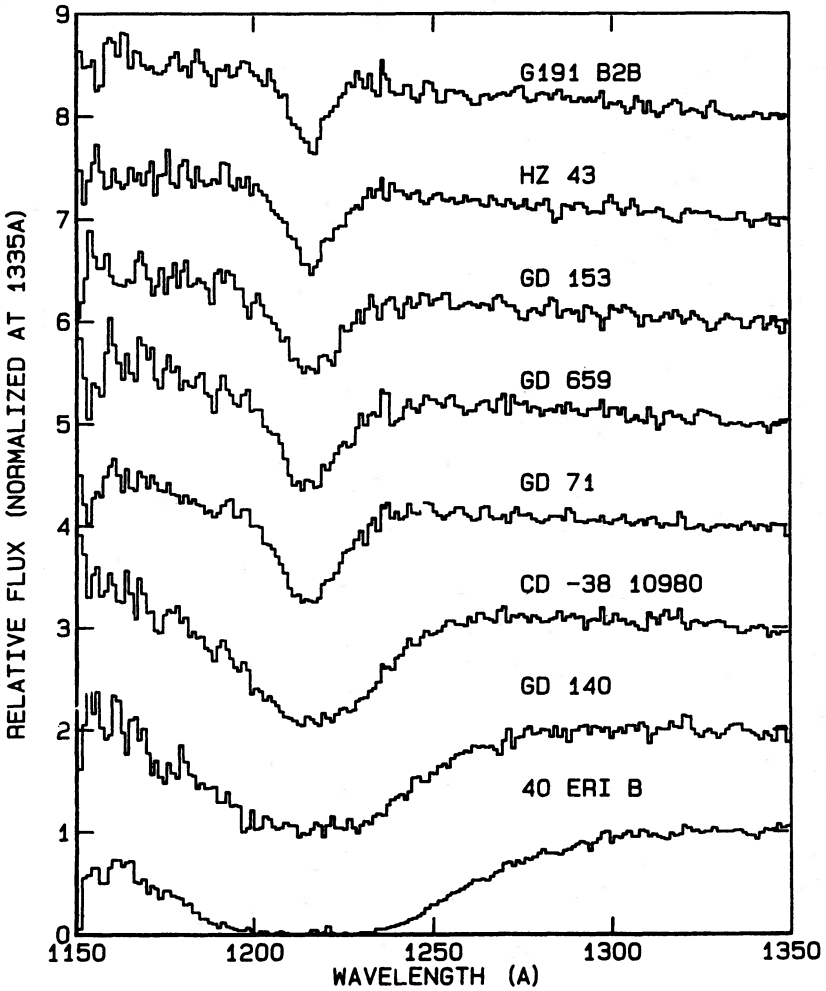

FIG. 1.—The development of the Lyα profile as a function of temperature. Small-aperture *IUE* fluxes are shown for a series of eight DA white dwarfs spanning a temperature range of 17,000–60,000 K. The spectra have been normalized to 1.0 at 1335 Å and offset from one another vertically. Temperatures derived from these profiles are given in Table 3.

TABLE 1

IUE OBSERVATIONS

Object/WD Number	SWP	Aperture	Effective Exposure Time(s)	Observer(s)[a]	Comments
40 Eri B/0413−077	23803	L/S	84/151	HW	
	10124	L/S	95/300	MS	small aperture double exposure
	7973	L	300	JG	trailed
	3741	L	300	JG	trailed reprocessed
Wolf 1346/2032+248	23814	L/S	340/660	HW	overexposure
	1650	L	299	JG	reprocessed
GD 140/1134+300	23220	—/S	—/720	HW	
	18996	L	900	GW	
CD −38°1980/1620−391	20340	L/S	110/220	JH	
	18291	L	120	CB	
	20370	L	93	FB	
GD 394/2111+498	23217	L/S	540/1200	HW	overexposed
	14296	L	449	WS	
GD 71/0549+158	23815	L/S	640/1140	HW	overexposed
	23804	L	690	HW	overexposed
	18272	L	300	CB	double exposure
GD 659/0050−332	20338	L/S	450/900	JH	
	†7013	L	1080	CB	double exposure
GD 153/1254+223	23219	L/S	600/1140	HW	
	11295	L/S	900/1800	HG	
	7448	L	900	DK	
HZ 43/1314+293	23218	L/S	380/795	HW	
	14500	L	300	TA	
	7221	L	300	SP	overexposed
	1528	L/S	420/420	KD	reprocessed
GD 246/2309+105	23802	L/S	310/620	HW	
	23216	L/L	270/600	HW	
	17011	L	360	CB	
G191−B2B/0501+527	23813	L/S	86/155	HW	
	23800	L/S	86/155	HW	
	15728	L	347	TA	trailed
	14602	L	82	TA	
	21817	L	94	CW	
Feige 24/0232+035	23801	L	205/390	HW	
	18215	L	100	FB	

[a] OBSERVERS.—(HW) Holberg and Wesemael. (MS) Savedoff. (JG) Greenstein. (GW) Wegner. (JH) Holberg. (CB) Basri. (FB) Bruhweiler. (WS) Malkan. (HG) Gursky. (DK) Koester. (TA) Ake. (SP) Selvelli. (KD) Hartmann. (CW) Grady.

Individual Lyα profiles employing any significant departure from a simple scaling of the small-aperture fluxes are discussed below.

40 Eri B.—Several previous SWP images of this star exist, including two small aperture images (SWP 23803 and 10124). Among these various spectra a considerable amount of variation is present in the 1150–1190 Å portion of the blue wing. Consequently several versions of the 40 Eri B Lyα profile were constructed from various combinations of large and small apertures. The one fitted best by the models and which is presented here consists of the average of the two small apertures scaled to the SWP 10124 large-aperture flux.

GD 140.—No simultaneous large- and small-aperture image was available for this star. It was therefore necessary to scale the existing small-aperture flux (SWP 23230) to a previous large-aperture (SWP 18996) image. This appears to have caused no problem since the spectral ratio of these two images was flat.

GD 71.—The red wing fluxes of both apertures in the 1250–1350 Å regions of SWP 23815 suffer from significant overexposure, which is evident in their ratio with SWP 18272. In order to avoid use of these fluxes we have constructed a composite profile using SWP 18272 fluxes longward of 1235 Å and scaled small-aperture SWP 23815 fluxes shortward.

GD 153.—The Lyα profile of this star was derived from the large- and small-aperture fluxes of SWP 23219. It was noticed that the Lyα profile in the small aperture was significantly redshifted in wavelength by ~ 2 Å. Reprocessing of the image failed to remove this shift or to provide an explanation for its presence. Unfortunately, the large-aperture Lyα profile is almost completely filled in by geocoronal emission, and it is not possible to determine if a similar shift is present. We note, however, that the large-aperture geocoronal feature appears to be in its correct position. Since the radial velocity implied by the small-aperture redshift is unrealistic, and no shift appears to be present in SWP 11295, we have applied an ad hoc wavelength shift to this star prior to fitting.

b) Visual Magnitudes

In addition to the *IUE* Lyα profiles of these stars, we also utilize their visual magnitudes. Our adopted V magnitudes for each star are given in Table 2. For 10 of our 12 stars, this quantity and its associated uncertainty is estimated directly from a simple weighted mean of the published V and Strömgren y magnitudes referenced in Table 2. Implicit in directly combining the results of V and y band photometry is the assumption that $V \equiv y$ and that magnitudes in the two systems constitute independent measurements of monochromatic flux

TABLE 2

ADOPTED VISUAL MAGNITUDES AND PREVIOUSLY DETERMINED TEMPERATURES

OBJECT	V		$T_{\rm eff}$(K)(σ_T)	
	Value	Reference	Value	Reference
40 Eri B	9.53 ± 0.01	1, 2, 3, 4, 5	16942 (190)	6
W1346	11.53 ± 0.01	1, 4, 7, 8, 9, 10	21002 (293)	6
GD 140	12.48 ± 0.05	1, 7, 10, 11, 12	21599 (282)	6
CD −38°10980	11.00 ± 0.01	2, 13, 14, 15, 16	24532 (653)	6
GD 71	13.04 ± 0.02	7, 11, 17, 18	34800 (1600)	28
GD 659	13.36 ± 0.02	13, 20, 21, 22	36354 (1776)	6
GD 394[a]	13.08 ± 0.02	10, 12, 23	33000 (3000)	24
GD 153	13.37 ± 0.02	1, 7, 8, 25, 26	40437 (1908)	6
GD 246	13.10 ± 0.01	7, 13, 17, 18, 26, 27	65000 (6402)	6
Feige 24	12.56 ± 0.05	See text	63000 (3000)	28
HZ 43	12.99 ± 0.03	See text	57500 (2500)	29
G191 B2B	11.79 ± 0.02	9, 30	56788 (3336)	6

[a] Originally designated "DO?" (Greenstein 1976).

REFERENCES.—(1) Graham 1972. (2) Wegner 1979. (3) Wegner and Schulz 1981. (4) Eggen and Greenstein 1965. (5) Eggen 1966. (6) Koester, Schulz, and Weidemann 1979. (7) Wegner 1983. (8) Lacombe and Fontaine 1981. (9) Routly 1972. (10) Schwartz 1972. (11) Eggen and Greenstein 1967. (12) Moffett, Barnes, and Evans 1978. (13) Bessell and Wickramasinghe 1978. (14) Hiltner, Stephenson, and Sanduleak 1968. (15) Greenstein 1970. (16) Wegner 1973. (17) Heckathorn and Opal 1985. (18) Landolt 1973. (19) Wesselius and Koester 1978. (20) Sanduleak and Philip 1968. (21) Rodgers 1971. (22) Eggen and Bessell 1978. (23) Bern and Wramdemark 1973. (24) Koester, Liebert, and Hege 1979. (25) Fontaine *et al.* 1985. (26) Eggen 1968. (27) Green 1980. (28) Wesselius and Koester 1978. (29) Malina, Bowyer, and Basri 1982. (30) Greenstein 1969.

at 5500 Å. The validity of the first part of this assumption can be established from those stars in our sample (except GD 140) which have been measured in both systems. For all 10 stars, except GD 140, the existing photometry is highly consistent and our adopted uncertainties are formal statistical errors. The case of GD 140 is puzzling in that existing photometry is highly discrepant. Eggen and Greenstein (1967) and Schwartz (1972) report V magnitudes of 12.50 and 12.60, respectively, while Wegner (1983) and Graham (1972) report y magnitudes of 12.37 and 12.46, respectively. Our adopted value of 12.48 includes an additional transformed V magnitude of 12.47 derived by Moffett, Barnes, and Evans (1978). In view of the disagreement over the visual brightness of this star, we adopted a cautious uncertainty of ±0.05 mag.

For two stars in our sample, HZ 43 and Feige 24, no reliable measurements of visual magnitude exist. In the case of HZ 43, the white dwarf (HZ 43A) is only 3″ from a red dwarf companion (HZ 43B). Existing HZ 43 colors (Eggen and Greenstein 1965; Landolt 1973) indicate V is contaminated by HZ 43B. We have taken two independent approaches to estimating the V magnitude of HZ 43. First, we have compared the Oke (1974) multichannel magnitudes for HZ 43 with those of G191 B2B. Oke reports that the tabulated HZ 43 results were free from contamination by HZ 43B. At 5500 Å, G191 B2B is found to be 1.207 ± 0.02 magnitudes brighter than HZ 43A, which implies a V of 13.00 ± 0.03 for HZ 43. Our second method is to consider *IUE* flux ratios of HZ 43 with GD 246 and G191 B2B, over the range 1150–3200 Å. Since the temperature differences involved are not large, these ratios are very nearly linear functions of wavelength on a log-log scale and can therefore be extrapolated to 5500 Å with considerable confidence. When this is done V magnitudes of 12.99 ± 0.07 and 12.93 ± 0.10 are obtained for HZ 43 from the flux ratios with GD 246 and G191 B2B, respectively. Considering both methods we adopt $V = 12.99 \pm 0.03$ for HZ 43. In the case of Feige 24 no visual separation is possible, and the Oke (1974) magnitudes show clear evidence of the red dwarf companion at wavelengths longward of 3900 Å. In this case we rely solely on *IUE* flux ratios of Feige 24, with G191 B2B, GD 246, and HZ 43. Proceeding in the same manner as with HZ 43 we find Feige 24 V magnitude estimates of 12.52 ± 0.13, 12.57 ± 0.11, and 12.58 ± 0.07 from extrapolations of the flux ratios with G191 B2B, GD 246, and HZ 43, respectively. Combining these results we obtain $V = 12.56 \pm 0.05$ for Feige 24. In addition to helping to estimate magnitudes for HZ 43 and Feige 24 the *IUE* flux ratios also provide a direct, calibration-independent, means of establishing accurate relative temperature differences between these four hottest stars in our sample. This will be discussed in greater detail in § V.

III. ANALYSIS

a) White Dwarf Model Atmospheres

The white dwarf model atmospheres employed here are pure hydrogen, blanketed models identical to those described in Holberg *et al.* (1985). Here, however, the model grid has been expanded to include temperatures between 16,000 and 70,000 K at gravities of $\log g = 8.5$, 8.0, and 7.5. An additional sequence of $\log g = 7.0$ models also covers the range 40,000–70,000 K. In total the grid contains 114 separate models, thus ensuring that Lyα profiles representing intermediate temperatures and gravities can be accurately interpolated. Each model contains a well-sampled, detailed synthetic Lyα profile computed in LTE using the unified Stark-broadening theory of Vidal, Cooper, and Smith (1973). In order to account for the spectral resolution of *IUE* low-dispersion spectra, we have smoothed the Lyα region (1150–1350 Å) of all models with a Gaussian having a full width at half-maximum of 5.75 Å. From the study of Cassatella, Barbero, and Benvenuti (1984), this resolution is characteristic of low-dispersion SWP data in the Lyα region. Inclusion of instrumental resolution is most important for the hottest stars (>40,000 K) where the Lyα profile narrows significantly.

b) Model Fitting

The procedures used to fit the observed Lyα profiles are similar to those discussed in Holberg *et al.* (1985). Basically, model profiles are interpolated from within our uniform grid, and a lattice of χ^2 values in the $T_{\rm eff}$–log g plane is computed for each observed profile. The resulting χ^2 values then determine the best fitting model and associated $T_{\rm eff}$–log g contours of equal confidence. The models are fitted on an absolute flux scale through normalization to the adopted V magnitude of each star. This normalization employs a conversion to monochromatic flux at 5500 Å based on an absolute flux of 3.57×10^{-20} ergs cm^{-2} s^{-1} Hz^{-1} from Vega at that wavelength (Tüg, White, and Lockwood 1977).

In order to investigate the effects of random errors and systematic biases on our results, we have fitted each observed profile using several different variations of the basic procedure described above. One method involved severing the link to the observed V magnitude by normalizing the models to their observed flux at 1310 Å. This, in effect, fits only to the overall shape of the profile and is insensitive to true absolute flux levels. The result of this procedure is a somewhat wider range of acceptable temperatures and gravities but no significant shifts in the locations of the best fitting models. A second method involved restricting the wavelength region over which the fit is performed so that approximately the same proportion of profile and continuum is considered for each star. This has the effect of lessening the relative weight given to continuum flux for hot stars such as HZ 43 and Feige 24 as opposed to cooler stars such as 40 Eri B and W 1346. All of the results discussed in this paper were obtained using this procedure. The standard adopted for the balance between profile and continuum is CD −38°10980 (see Fig. 4*a*). Thus, for all stars hotter than CD −38°10980, wavelength ranges were reduced in portion to the measured equivalent widths of the Lyα profile. For the three cooler stars the full 1150–1350 Å window was employed.

In addition to these variations in the fitting procedure, we have also investigated the sensitivity of our results to uncertainties in the adopted V magnitudes. Since these uncertainties enter through the normalization they can just as well be regarded as measures of the sensitivity of our results to any *systematic* uncertainty in the *IUE* absolute calibration between 1200–1350 Å. These sensitivities are expressed in Table 3 as partial rates of change of $T_{\rm eff}$ per magnitude V.

c) Statistics and Treatment of Errors

Part of the process of constructing the Lyα profiles which we have analyzed involved estimating the random component of the *IUE* photometric errors. This was done by approximating each observed profile with a cubic spline. Individual *IUE* flux points were then assigned an uncertainty computed from the mean variance, with respect to the spline for all points within ±5 Å. This was done at the original *IUE* sampling resolution of ~1.2 Å and was assumed to represent a "1 σ" error for each flux point. The subsequent χ^2 values determined during our analysis included these errors and were based on approximately 160 *IUE* flux samples for each 200 Å wide Lyα profile. Since the actual SWP spectral resolution is 5–6 Å, this represents a significant oversampling of the data. In order to account for this oversampling we have employed the 5.75 Å spectral resolution, used to smooth the models, and assumed that each profile is composed of up to 200/5.75 = 34 "independent samples." This in turn yields a maximum of ~32 effective degrees of freedom for each model fit, after allowing for the deletion of several flux points in each profile. A further reduction in the effective degrees of freedom result from the diminished wavelength ranges used to preserve the profile to continuum ratio for the hotter stars (§ III*b*). The confidence intervals displayed in Figure 2 are determined from χ^2/ν (~160) *but* are evaluated for the appropriate effective degrees of freedom. These effective degrees of freedom are given along with χ^2/ν in Table 3.

In examining our profiles it was clear the first several samples of each spectrum ($\lambda \approx 1150$ Å) were meaningless. These were effectively deleted from our sample by assigning them very large errors (zero weight). Likewise, it was also decided that the core of the Lyα profile was subject to large uncertainties due to residual geocoronal Lyα (only really apparent in GD 394), interstellar H I absoprtion, and unmodeled non–LTE core effects. In order to deal with these issues, the central sample of each profile was also given zero weight. In one case, GD 394, it was apparent substantial geocoronal contamination was present and the four central core samples were assigned zero weight.

d) Modifications to IUE Fluxes

Initial fits to all 12 stars in our sample produced acceptable temperatures and gravities but yielded reduced χ^2's in excess of 2. Comparisons with the observed profiles showed an excess

TABLE 3

FINAL RESULTS

Object	$T_{\rm eff}$(K)(σ_T)	log (g)(σ_g)	$R^2/D^2 \times 10^{23}$	$\chi^2/\nu(\nu)$	$\partial T/\partial V \times 10^{-3}$ (K)	W_{30}(Å)(σ_w)	W_{30}(Å)(σ_w)
40 Eri B	16325 (325)	7.65 (0.20)	368.00	6.34 (28)	3.5	42.85 (1.57)	67.41 (1.83)
W1346	20680 (210)	8.08 (0.15)	39.80	1.08 (30)	9.4	36.65 (1.66)	54.61 (2.01)
GD 140	21375 (395)	8.45 (0.15)	15.80	1.30 (33)	6.0	38.52 (1.62)	58.59 (1.91)
CD −38°10980	24500 (140)	8.08 (0.15)	50.30	1.07 (32)	10.0	30.92 (1.07)	44.46 (1.33)
GD 71	33300 (830)	7.78 (0.20)	4.22	1.04 (19)	33.1	17.05 (0.67)	20.76 (0.70)
GD 394	36125 (940)	8.13 (0.25)	3.68	0.93 (14)	33.3	13.03[a]	17.46[a]
GD 659	36850 (1390)	8.17 (0.30)	2.73	0.81 (17)	34.4	15.19 (0.66)	20.74 (0.81)
GD 153	42375 (1480)	8.23 (0.30)	2.73	0.87 (12)	57.5	12.43 (0.54)	14.98 (0.57)
GD 246	53600 (2940)	7.64 (0.45)	2.43	0.98 (12)	80.0	6.97 (0.40)	10.03 (0.45)
Feige 24	55000 (5360)	7.23 (0.35)	4.01	1.12 (9)	82.5	6.60 (0.35)	9.35 (0.35)
HZ 43	57500 (3310)	8.5	2.55	1.08 (10)	87.5	8.14 (0.39)	6.74 (0.39)
G191 B2B	62250 (3520)	7.55 (0.35)	7.25	1.04 (9)	83.9	5.59 (0.32)	7.28 (0.32)

[a] Core of profile contains geocoronal Lyα emission.

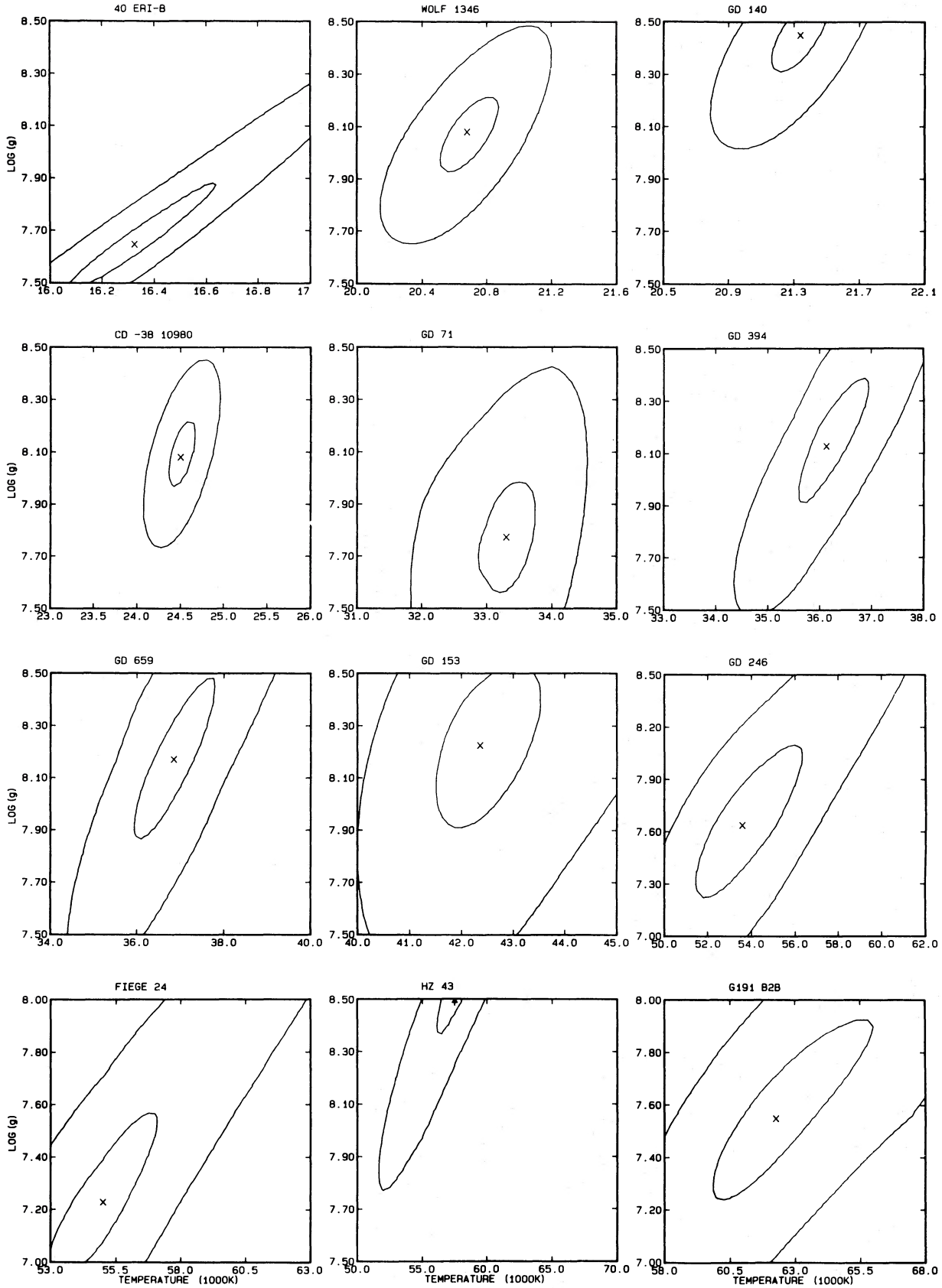

FIG. 2.—Contours of equal χ^2 for the 12 stars in our sample. Temperatures and gravities corresponding to best-fit models are indicated by χ's. Also shown are 1 σ and 2 σ contours of equal χ^2.

with respect to the best fitting models in a region centered on 1275 Å. This "red wing excess" has been previously noted by Holberg *et al.* (1985) and is illustrated in Figure 1 of that reference. It was suggested at the time that this effect might be due to a wavelength-dependent undulation in the *IUE* calibration or perhaps due to departures from the line-broadening theory used in the models. With the present observations, covering a wide range of effective temperatures, we are in a position to resolve this issue.

We have ratioed our best-fitting models to the observed profiles over the range 1150–1350 Å for all stars in our sample, excluding 40 Eri B (this star is not included for reasons which will be discussed later). Ignoring a ~14 Å wide region in the vicinity of Lyα, where line saturation can cause signal-to-noise ratio problems, we find all resulting ratios exhibit a similar wavelength dependence. These ratios and their mean are plotted in Figure 3 and show no evidence of temperature dependence even though the stars in question range from 20,000 K to 60,000 K and have corresponding equivalent widths ranging from 50 Å to 6 Å. Any unmodeled broadening-related effect would not be expected to remain temperature independent over this range. We therefore attribute this effect to the *IUE* absolute calibration. We have employed the SWP calibration defined in Bohlin and Holm (1980) as our reference and will discuss our proposed modification relative to that standard.

In what follows we will consider the influence our modification has on our results within the 1150–1350 Å Lyα window. Extension of these results to include the entire SWP wavelength range will be presented elsewhere. We have applied a correction to our observed fluxes based on the mean ratio shown in Figure 3, in the sense that the observed fluxes have been divided by the ratio. These corrected fluxes are refitted to the models in exactly the same manner as before. The resulting reduced χ^2's were significantly lower, clustering about 1. The best-fit temperatures, however, are *not* significantly influenced by use of the modified fluxes. For example, initial uncorrected fluxes yielded a best-fit temperature of 24,700 K for CD −38°10980 (Holberg *et al.* 1985). Inclusion of corrected fluxes shifts this temperature by only 200 K to 24,500 K. In general changes in temperature were less than 1%. This insensitivity of effective temperature to application of the red wing correction indicates that it introduces no significant temperature biases. Gravities, on the other hand, are influenced, with the mean gravity of the entire sample decreasing by 0.15. Given our low sensitivity to gravity and the fact that it is largely uncorrelated with temperature, this is not a significant change.

Previous investigators (Hackney, Hackney, and Kondo 1982; Finley, Basri, and Bowyer 1984) have also proposed modifications to the *IUE* absolute calibration. We comment briefly here on how our results relate to these efforts. Hackney, Hackney, and Kondo investigated wavelength- and exposure-related features ("continuum distortion") in low-dispersion SWP images. They considered objects with power-law–like energy distributions (BL Lac objects and the sdO star BD +28°4211) over the wavelength range 1250–1930 Å. From residuals to power-law fits, they determined a wavelength-dependent correction vector. Over the limited range (1250–1350 Å) where the Hackney, Hackney, and Kondo results overlap ours, they show a similar, but significantly shallower increase than we find. Finley, Basri, and Bowyer investigated wavelength- and time-dependent modifications to the absolute fluxes of both SWP and LWR cameras over the range 1300–3200 Å. As we do, they consider model atmosphere fluxes for a series of DA white dwarfs relative to observed *IUE* fluxes. They began with temperature estimates derived from the

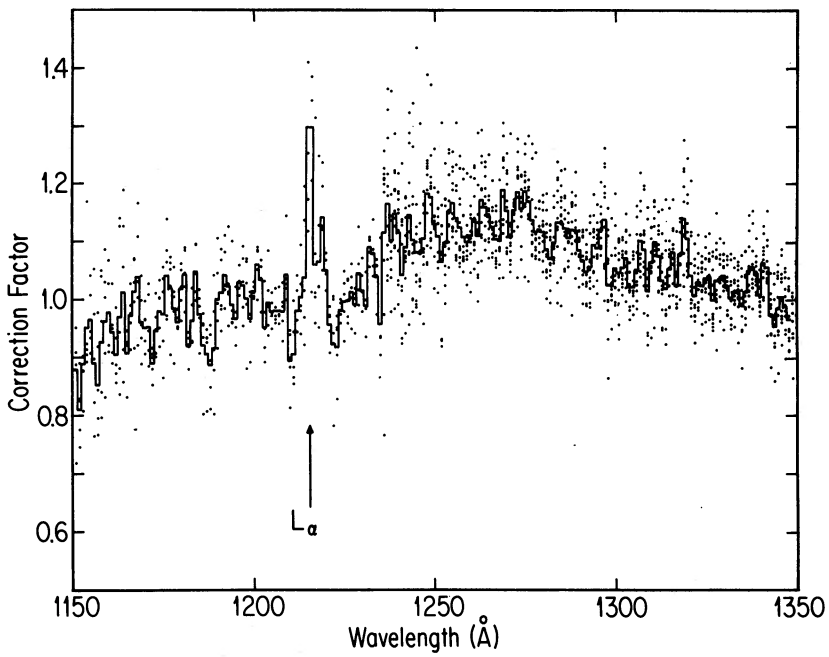

FIG. 3.—The correction factor applied to the *IUE* fluxes. The heavy histogramed line is the mean of 11 individual corrections whose scatter is indicated by the dots. In determining individual correction factors, the 1150–1350 Å fluxes for each star were divided by the best-fitting model. For the cooler stars in our sample, the center of the Lyα profile contains very little flux, and the division by the models generates relative large errors. Therefore, for the six coolest stars ($T < 40{,}000$ K), we have only considered correction factors longward of 1236 Å. For the remaining five hotter stars, we consider the entire 1150–1350 Å region. Even for these stars the center of the Lyα feature exhibits an approximately ~14 Å wide self-reversed artifact centered on 1216 Å.

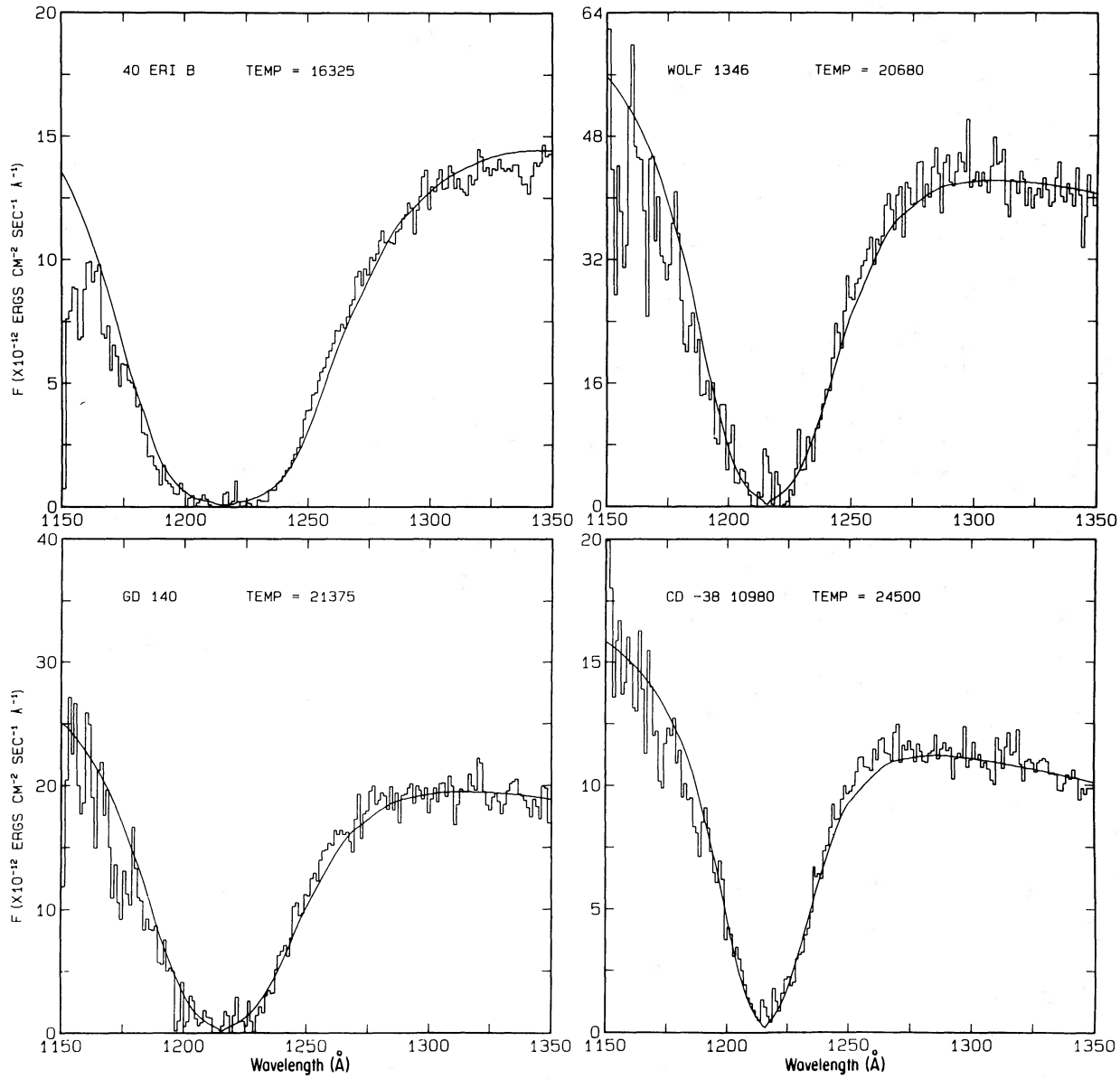

FIG. 4*a*

FIG. 4.—Observed Lyα profiles of the 12 stars in our sample compared to the best-fitting models

published optical colors for their stars and sought wavelength- and time-dependent correction vectors which provided a self-consistent set of temperatures and *IUE* flux modifications. There is not sufficient wavelength overlap between our two results for meaningful comparison; however, several general comments can be made concerning both results. We have assumed no changes in the SWP sensitivity with time. While this is not strictly true, it is a good approximation over the limited 200 Å window we are considering (R. C. Bohlin, private communication). Results from *IUE* sensitivity monitoring programs (Holm 1985; Sonneborn and Garhart 1983) generally show changes to be the strongest in the mid-UV between 1500 and 2500 Å and negligible at 1300 Å. We also use an internally self-consistent set of observed temperatures to derive our flux modifications. Ideally, extension of our results to the entire SWP and LWR wavelength range would first involve correcting the *IUE* fluxes to a standard epoch using the results of the *IUE* sensitivity monitoring program. This is already possible for the LWR at a reasonable wavelength resolution and should be possible for the SWP. Wavelength-dependent corrections should then be available with respect to a self-consistent set of model temperatures derived from Lyα profile fits.

e) Final Results

Our final results, presented in Table 3, consist primarily of the three quantities necessary to completely describe each model; effective temperature ($T_{\rm eff}$), surface gravity (log g), and solid angle (R^2/D^2). In Table 3 these quantities correspond to the best-fitting models discussed previously and are the parameters used to generate the fits shown in Figures 4*a*, 4*b*, and 4*c*. The solid angle used here refers to the normalization param-

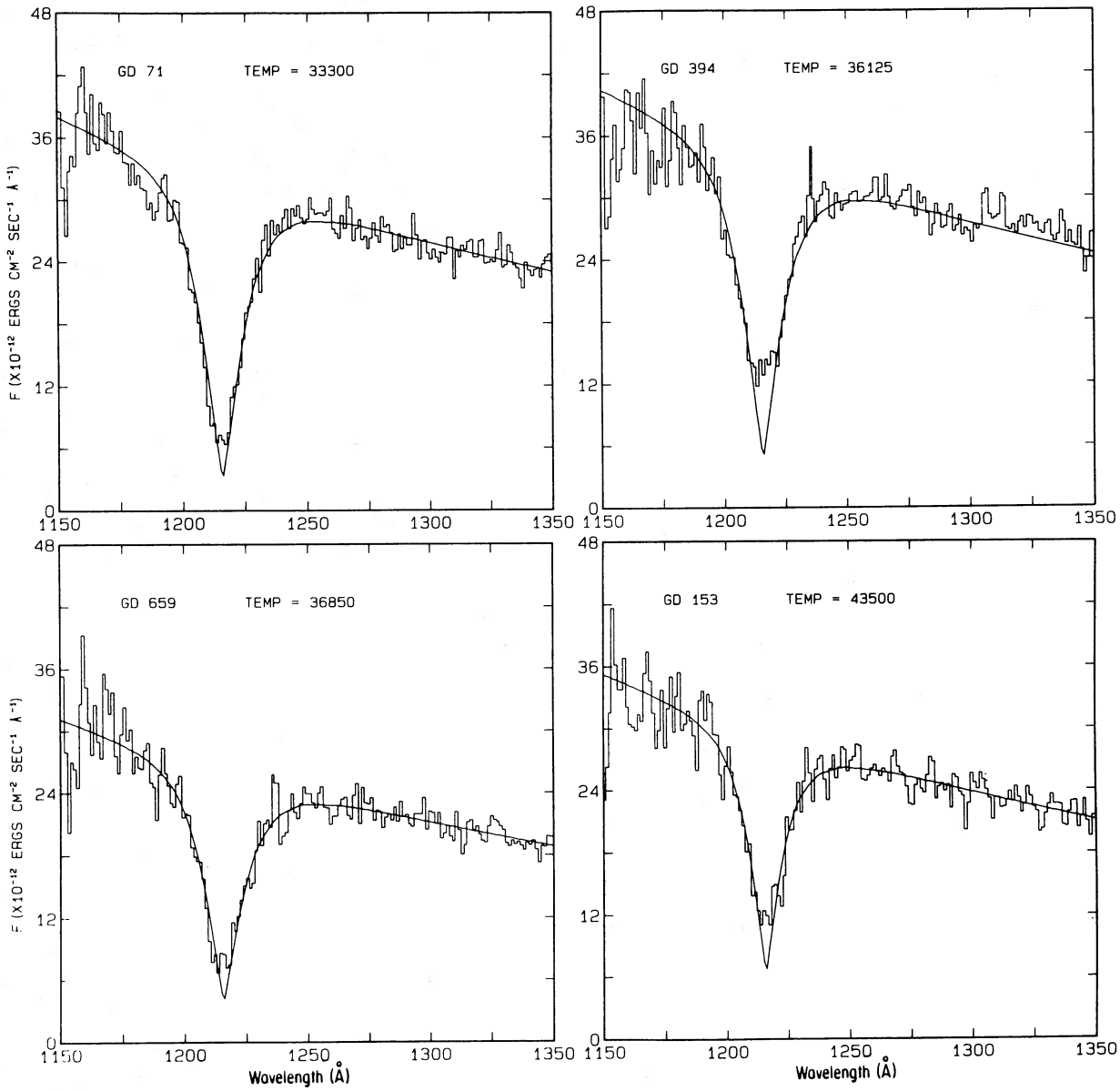

FIG. 4*b*

eter which relates the observed flux f_ν(ergs cm^{-2} s^{-1} Hz^{-1}) to the emergent Eddington flux H_ν(ergs cm^{-2} s^{-1} Hz^{-1} str^{-1}) of the model through the fundamental relation

$$f_\nu = 4\pi H_\nu R^2/D^2 \,. \quad (1)$$

Associated with the effective temperature is an uncertainty (σ_T) which is the Pythagorean sum of error components due to the Lyα fitting procedure and the adopted uncertainty in the visual magnitude (Table 2). Since determination of surface gravity is not a primary goal of this work, the corresponding surface gravity uncertainty (σ_g) is simply estimated from the 1 σ contours in Figure 2. Also provided in Table 3 are secondary parameters associated with the best fitting models and observed profiles. These are the minimum χ^2 per degree of freedom ($\chi_{\min}{}^2/\nu$), the effective degrees of freedom for each profile (ν), temperature sensitivity per unit magnitude of observed visual flux ($\partial T/\partial V$), and two measures of observed equivalent width (W_{30}, W_{50}). The latter are not true equivalent widths but are pseudo–equivalent widths evaluated at fixed distances (± 30 and ± 50 Å) from line center in accord with the definition given in Wesemael *et al.* (1980).

IV. DISCUSSION

It is of considerable interest to compare our final temperatures with those previously estimated by other means; these estimates are contained in Table 2. In an effort to maintain homogeneity, we have relied as much as possible on the ground-based results of Koester, Schulz, and Weidemann (1979) who determined temperatures for all our stars with the exception of GD 71 and GD 394. For these stars we have employed the *ANS* results of Wesselius and Koester (1978) and the optical results of Koester, Liebert, and Hege (1979), respec-

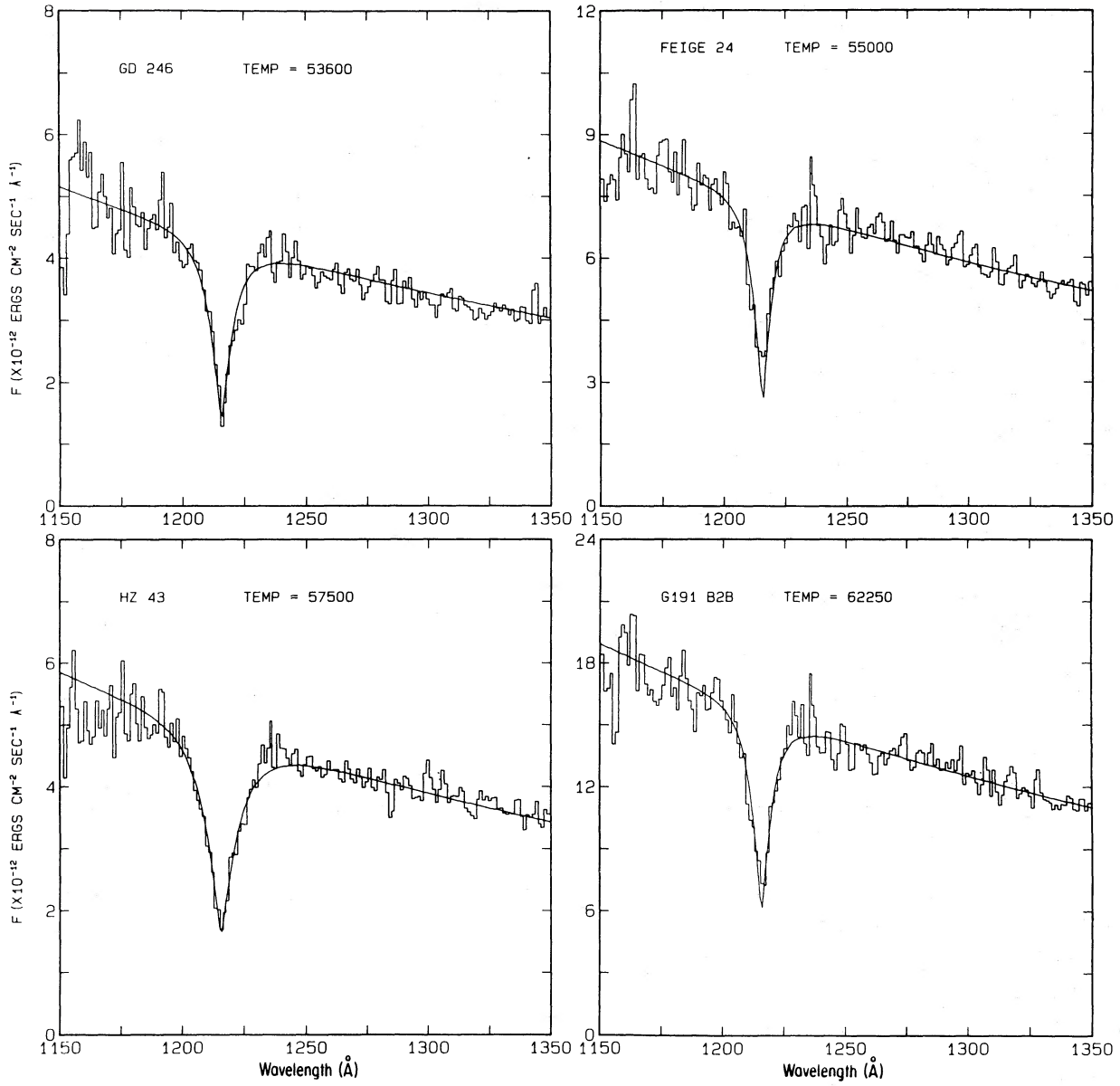

FIG. 4*c*

tively. For two additional stars, HZ 43 and Feige 24, the Koester, Schultz, and Weidemann temperatures are not applicable, since the photometric contamination of the M dwarf companions appear not to have been taken into account. For these two stars we use the estimates of Malina, Bowyer, and Basri (1982) and Wesselius and Koester (1978) for HZ 43 and Feige 24, respectively. In Figure 5, we directly compare results with these given in Table 2. As can be seen the agreement between these two sets of results is very good with the majority of stars agreeing to within their mutual uncertainties. This is an indication that no significant biases exist between these two sets of results.

In spite of the fact that our fits do not provide a sensitive determination of surface gravity, we believe there are several significant conclusions which can be drawn from these results. First, as expected most of our results cluster about log $g = 8.0$. A simple mean of the gravities in Table 2 yields a value of 7.96 with a standard deviation of 0.37, values not significantly different from those found by Koester, Schulz, and Weidemann (1979) from a much larger sample. It has been pointed out by several authors that the hottest white dwarfs may be expected to have lower than average gravities due to radii which are larger than those given by standard zero temperature mass-radius relationships. The largest such effects are predicted by the models of Koester and Schonberner (1985) which invoke residual hydrogen burning in the stellar envelope. Such a systematic trend may be present in our data, where three of our four hottest stars have gravities significantly less than 8.0. An obvious exception to this result is HZ 43, which has the highest gravity in our sample. We discuss the particular case of HZ 43 and the other anomalous high-gravity star, GD 140, in more detail.

HZ 43.—The surface gravity we obtain for HZ 43 is surprisingly high, in fact, the best-fitting result lies just outside our

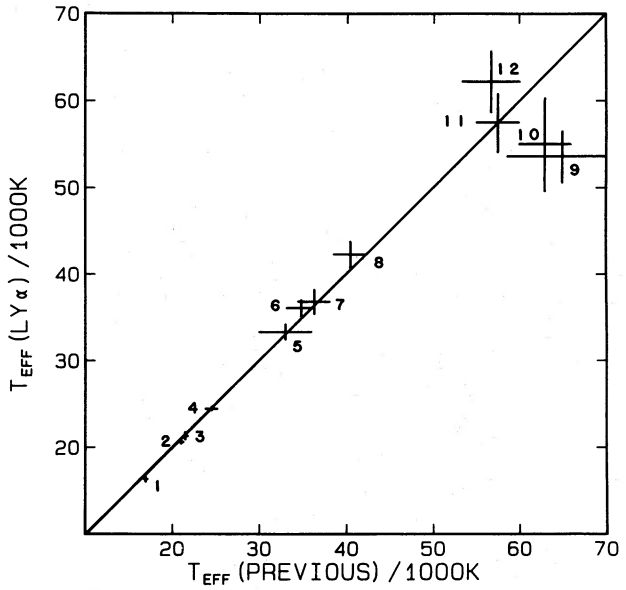

FIG. 5.—A comparison of effective temperatures determined from Lyα profiles with those determined primarily from ground-based photometry. Individual stars are numbered according to their order of presentation in the text: (1) 40 Eri B; (2) W1346; (3) GD 140; (4) CD −38°10980; (5) GD 71; (6) GD 659; (7) GD 394; (8) GD 153; (9) GD 246; (10) Feige 24; (11) HZ 43; (12) G191 B2B.

grid as can be seen in Figure 2. The best-fitting temperature on the other hand is well within the range of a number of previous estimates based on soft X-ray (Heise 1984; Auer and Shipman 1977), EUV (Holberg *et al.* 1980; Malina, Bowyer, and Basri 1982) and ultraviolet (Wesselius and Koester 1978) observations. Can the gravity of HZ 43 be well in excess of 8.0 given by the expectation of the hottest white dwarfs have lower than average gravities? Using our solid angle (Table 3) and the relatively well-established parallax for HZ 43 ($\pi = 0''.0158 \pm 0''.003$; Dahn *et al.* 1982; Margon *et al.* 1976) and assuming the mass-radius relation (Hamada and Salpeter 1961) for a carbon/oxygen composition core, it follows that the gravity of HZ 43 cannot exceed 8.08. Such a value is approximately 1.5 σ from our best-fit value. A careful comparison of the HZ 43 Lyα profile with the profiles of the other three hot DAs shown in Figure 4*c*, however, leads to the inescapable conclusion that the HZ 43 profile is significantly broader than the others, implying a higher gravity. This is also evident from the equivalent widths tabulated in Table 3. It should be mentioned, however, that with the exception of rotation, which does not change equivalent width, a modest magnetic field could also broaden the Lyα line. Several hot DAs are known (Liebert *et al.* 1983) which exhibit such an effect.

There are two pieces of circumstantial evidence which also suggest HZ 43 may have a higher than average gravity. No trace of weak sharp-lined metallic features is seen in *IUE* high-dispersion spectra of HZ 43 (Bruhweiler and Kondo 1983). This is in contrast to the dozen or so DAs which do show the presence, or probable presence, of such features (F. C. Bruhweiler, private communication). One possible explanation for the existence of such features is a radiative acceleration which counteracts gravitational diffusion for selected metallic ions. Under this scenario, high gravities and less intense radiation fields (low temperatures) would favor the absence of such ions through diffusive loss. In fact, it can be argued that of the six DAs, including HZ 43, which are not known to show metallic features, all but one (EG 118) has either a high gravity (e.g., Sirius B, 8.65) or a low temperature (e.g. 40 Eri B, 16,900 K). An additional line of evidence involves the low limits which soft X-ray observations (Petre, Shipman, and Canizares 1986; Heise 1984) place on the He abundance [n(He)/n(H) $< 10^{-5}$] in the atmosphere of HZ 43. Petre, Shipman, and Canizares present strong evidence that the atmospheric He abundance in DA white dwarfs tend to increase with temperature and argue that this can be explained by radiative acceleration effects which would also presumably explain the presence of the metallic lines. The outstanding exception to this trend is HZ 43. These authors suggest that this exception can be explained if HZ 43 has a high mass and hence a high gravity. Better estimates of the gravity of HZ 43 will hopefully be available from analysis of the Balmer profiles. Until that time, however, our gravity estimate rests on a single HZ 43 small-aperture Lyα profile. Attempts should be made to reobserve HZ 43 in order to confirm this result.

One potentially observable consequence of a relatively massive HZ 43, which is not seen, is remnant nebulosity from the precusor planetary nebula phase. Such a massive central star would evolve rapidly and subsequently eject a more massive nebulae.

GD 140.—The other star in our sample with a high gravity is GD 140 with a value of 8.45 ± 0.15. Again, inspection of the profile and considerations of its measured equivalent widths (Table 3) indicate an abnormal breadth for its temperature. In addition to their temperature estimate, Koester, Schulz, and Weidemann (1979) also find a high surface gravity (8.79 ± 0.16) for this star and remark on its uniqueness in their sample of DAs. It is also perhaps significant that GD 140 is among the DAs *not* found to show sharp narrow-lined metalic features (F. C. Bruhweiler, private communication). The minimum mass for GD 140 consistent with our solid angle and minimum gravity (8.30) and the parallax of $\pi = 0''.046 \pm 0''.006$ quoted in Koester, Schulz, and Weidemann, is 0.83 $M_{\odot}$.

One effect which could conceivably affect our temperature estimates is the existence of small amounts of interstellar reddening along our lines of sight. All of our stars lie within 100 pc, and it is possible that extinctions of $E(B-V) \leq 0.02$ may exist and have escaped notice. Although we have no independent means of determining the existence of small amounts of reddening, we note that in several instances stars in our sample are known to be EUV and strong soft X-ray sources, implying very low interstellar H I column densities and by inference insignificant extinctions. These stars are HZ 43, GD 153, and G191 B2B (Holberg 1984). All results presented in Table 3 assume *no* interstellar reddening.

The most unsatisfactory of all our results is that obtained for 40 Eri B, where χ^2/ν is 6.3. Although the fit to the 40 Eri B data shown in Figure 4*a* appears adequate to the eye over most of the profile, an unexpectedly large amount of variance is present in both the red and blue wings. Various schemes were employed to improve the fit, such as giving zero weight to fluxes in the extreme blue and red portions of the wing. While it was possible to somewhat reduce χ^2/ν, none of these attempts produced an acceptable result. It is possible that the relatively poor fits to the 40 Eri B data could be related to the presence of the recently identified satellite H I Lyα features (Nelan and Wegner 1985; Koester *et al.* 1985). A broad shallow absorption centered at 1405 Å due to a satellite line of the hydrogen ion (H_2^+) quasi molecule has been observed in a

number of moderate temperature DA white dwarfs (Wegner 1984); including 40 Eri B[2] (Greenstein 1980).

In spite of the fact that the 1405 Å feature does not appear to extend significantly into our Lyα window shortward of 1350 Å, it is reasonable to expect that satellite features may have a residual influence on the Lyα red wing. As a significant source of opacity the H_2^+ quasi molecule could influence the temperature structure. Indeed Nelan and Wegner have found that their computed emergent UV fluxes can be significantly affected by the presence of satellite lines in model calculations. Since our models do not incorporate such effects, it is also likely that they do not correctly reflect emergent fluxes in the vicinity of Lyα for 40 Eri B. In any case, the influence of these satellite features should vanish at temperatures in excess of 19,000 K (Nelan and Wegner 1985; Koester *et al.* 1985). Indeed our fits for W1346 (20,680 K) and GD 140 (21,375 K) are acceptable. In light of the difficulty in satisfactorily fitting 40 Eri B, the temperature and gravity tabulated for this star in Table 3 may be dominated by large external biases. This conclusion is strengthened by comparisons with the results of Wegner (1980) which fairly reliably establish a temperature of 16,900 K and a gravity of 7.86 ± 0.2. It would, of course, be interesting to determine if the inclusion of the opacity of quasi-molecular H_2^+ would lead to a better fit to the observed Lyα profile.

The four hottest stars in our sample (see Fig. 4*c*) all yield similar temperatures in the range 50,000–60,000 K. Since these four stars are widely regarded as among the hottest known DA white dwarfs, the obvious question arises as to whether ~60,000 K represents an observational upper limit to the temperature of stars which can be unambiguously classified as DA white dwarfs? The answer to this question is not clear. Fleming, Liebert, and Green (1986) have found six examples in the Palomar-Green survey (Green, Schmidt, and Liebert 1986) which they classify as DAs and to which they assign luminosities of $M_v = 7.7$ and temperatures in the range 70,000–100,000 K on the basis of their Hβ strengths. Direct comparison of the Balmer profiles of these objects with G191 B2B, HZ 43, and GD 246 indeed show tham to have significantly weaker and narrower Hγ and Hδ profiles indicating higher temperatures and/or lower gravities. Whether these stars meet the traditional log $g \geq 7.0$ criteria for white dwarfs is open to question. Also uncertain is their atmospheric composition. From the lack of any apparent He II λ4686 feature, a helium abundance of $n(\mathrm{He})/n(\mathrm{H}) \leq 10^{-3}$ (Wesemael, Liebert, and Green 1984) can be deduced. Further observation may well reveal the presence of He or other metals. They may well represent transitional objects, contracting toward white dwarf radii and having gravities between 6.0 and 7.0. These six stars are all fainter than 15th mag.

In spite of the fact that our four hottest stars have the largest uncertainties, we can provide some rather good *relative* temperatures for these stars. In § III we used *IUE* flux ratios of these stars to help estimate *V* magnitudes for HZ 43 and Feige 24. One useful by-product of this effort is that the slopes of the resulting spectral ratios establish differential temperatures between these stars. In constructing the ratios we proceeded as follows. For each star, the SWP images were co-added and combined with a single LWR image. The latter were corrected for the known time dependence (Holm 1985) of the LWR camera sensitivity. The resulting 1150–3200 Å energy distributions were then smoothed and regions including known artifacts and the Lyα profiles were removed. Simple linear regressions were then performed in the various ratios on a m_λ–log λ scale over the entire wavelength range. In Table 4 we provide SWP and LWR image numbers, the slopes of the spectral ratios, and resulting differential temperatures. All of the comparisons in Table 4 are made relative to HZ 43, which for this purpose we assume to have a temperature of 55,000 K.

In summary, we have satisfactorily fitted the *IUE* Lyα profiles of 11 out of a total of 12 DA white dwarfs and determined effective temperatures for these stars over a range of 20,000–60,000 K. These results are seen to be in good agreement with previous temperature estimates and provide a substantial improvement in the DA temperature scale over this range of temperatures. The hottest known DA is found to be G191 B2B (62,250 ± 3,520 K). Hotter DAs may exist, but their temperatures, gravities, and atmospheric compositions are currently not firmly established. In addition, these results demonstrate DA model atmsopheres to be a fairly precise tool for the determination of atmospheric parameters over a wide range of wavelengths. The failure to adequately fit our lowest temperature star may indicate an important qualification to the previous statement and the need to include additional quasi-molecular opacity sources in DA model atmospheres below 20,000 K. An additional by-product of our investigation has been proposed a modification to the *IUE* calibration valid over the wavelength range 1150–1350 Å. Simultaneously determined surface gravities, while not as accurate as those which will be forthcoming from the detailed analysis of Balmer profiles, indicate hotter DAs possess lower than average gravity. Finally, the two stars in our sample with the highest gravities, HZ 43 and GD 140, are consistent with a simple picture of the radiative support of He and heavier ions in the atmospheres of DA white dwarfs.

[2] The existence of additional satellite features at 1233.5 and 1240.5 Å is also predicted (Stewart, Peek, and Cooper 1973). We have searched for the presence of these additional features in various averages of the low-dispersion SWP images 23803, 10124, 7973, and 3741 and in the high-dispersion image SWP 7972. No evidence of these features was found at an equivalent width upper limit of 0.3 Å.

TABLE 4

IUE SPECTRAL RATIOS AND DIFFERENTIAL TEMPERATURES

Star	SWP	LWR	Slope[a]	$\Delta T_{HZ\,43}$[b]
GD 246	1701, 23802, 23216	13287	−0.059 (0.020)	−3800 (1300)
Feige 24	18215, 23801	3325	−0.044 (0.019)	−2800 (1200)
HZ 43	7221, 14500	6224	1	0
G191 B2B	14602, 15728	11200	0.225 (0.026)	+14400 (1600)

[a] Slope: mag (λ)/log (λ).

[b] $\Delta T_{HZ\,43}$: Differential temperature relative to HZ 43, assuming T_{eff} for HZ 43 of 55,000 K.

The authors would like to thank J. Liebert for a number of valuable comments. Archival *IUE* material provided by the National Space Science Data Center, NSSDC/WDC-A, is gratefully acknowledged. This work was supported by NASA grant NAG5-434 and by the NSERC Canada.

REFERENCES

Auer, L. H., and Shipman, H. L. 1977, *Ap. J. (Letters)*, **211**, L105.
Bern, K., and Wramdemark, S. 1973, *Lowell Obs. Bull.*, **161**, 1.
Bessell, M. S., and Wickramasinghe, D. T. 1978, *M.N.R.A.S.*, **182**, 275.
Bohlin, R. C., and Holm, A. 1980, *IUE Newsletters*, No. 10, p. 37.
Bruhweiler, F. C., and Kondo, Y. 1981, *Ap. J. (Letters)*, **248**, L123.
———. 1983, *Ap. J.*, **269**, 657.
Cassatella, A., Barbero, J., and Benvenuti, P. 1984, *IUE Newsletter*, No. 24, p. 84.
Dahn, C. C., *et al.* 1982, *A.J.*, **87**, 419.
Eggen, O. J. 1966, *Royal Obs. Bull. E*, No. 120, p. 333.
———. 1968, *Ap. J. Suppl.*, **16**, 97.
Eggen, O., and Bessell, M. S. 1978, *Ap. J.*, **226**, 411.
Eggen, O., and Greenstein, J. L. 1965, *Ap. J.*, **141**, 83.
———. 1967, *Ap. J.*, **150**, 927.
Finley, D. S., Basri, G., and Bowyer, S. 1984, in *Future of Ultraviolet Astronomy Based on Six Years of IUE Research*, ed. Y. Kondo, R. D. Chapman, and J. M. Mead (NASA CP-2349), p. 249.
Fleming, T. A., Liebert, J., and Green, R. F. 1986, *Ap. J.*, in press.
Fontaine, G., *et al.* 1985, *A.J.*, **90**, 1094.
Graham, J. A. 1972, *A.J.*, **77**, 144.
Green, R. F. 1980, *Ap. J.*, **238**, 685.
Green, R. F., Schmidt, M., and Liebert, J. 1986, *Ap. J. Suppl.*, **61**, 305.
Greenstein, J. L. 1969, *Ap. J.*, **158**, 281.
———. 1970, *Ap. J. (Letters)*, **162**, L55.
———. 1976, *A.J.*, **81**, 323.
———. 1980, *Ap. J. (Letters)*, **241**, L89.
Hackney, R. L., Hackney, K. R. H., and Kondo, Y. 1982, in *Advances in Ultraviolet Astronomy: Four Years of IUE Research*, ed. Y. Kondo, J. M. Mead, and R. D. Chapman (NASA CP-2238), p. 335.
Hamada, T., and Salpeter, E. E. 1961, *Ap. J.*, **134**, 683.
Heckathorn, H., and Opal, C. 1985, *Bull. AAS*, **16**, 966.
Heise, J. 1984, presentation at 18th ESLAB Symposium on X-ray Astronomy.
Hiltner, W. A., Stephenson, C. B., and Sanduleak, N. 1968, *Ap. Letters*, **2**, 153.
Holberg, J. B. 1984, in *IAU Colloquium 81, Local Interstellar Medium*, ed. Y. Kondo, F. C. Bruhweiler, and B. D. Savage (NASA CP-2345), p. 91.
Holberg, J. B., Sandel, B. R., Forrester, W. T., Broadfoot, A. L., Shipman, H. L., and Barry, D. C. 1980, *Ap. J. (Letters)*, **242**, L119.
Holberg, J. B., and Wesemael, F. 1984, in the *Future of Ultraviolet Astronomy Based on Six Years of IUE Research*, ed. J. Mead, R. D. Chapman, and Y. Kondo (NASA CP-2349), p. 285.
Holberg, J. B., Wesemael, F., Wegner, G., and Bruhweiler, F. C. 1985, *Ap. J.*, **293**, 294.
Holm, A. 1985, *IUE Newsletter*, No. 26, p. 11.
Iben, I., and Tutukov, A. V. 1984, *A. J.*, **282**, 615.
Kahn, S. M., Wesemael, F., Liebert, J., Raymond, J. C., Steiner, J. E., and Shipman, H. 1984, *Ap. J.*, **278**, 255.
Koester, D., Liebert, J., and Hege, E. K. 1979, *Astr. Ap.*, **71**, 163.
Koester, D., Schulz, H., and Weidemann, V. 1979, *Astr. Ap.*, **76**, 262.
Koester, D., and Schonberner, D. 1985, *Astr. Ap.*, in press.
Koester, D., Weidemann, V., Zeidler-K. T., E.-M., and Vauclair, G. 1985, *Astr. Ap.*, **142**, L5.
Lacombe, P., and Fontaine, G. 1981, *Astr. Ap. Suppl.*, **43**, 367.
Landolt, A. U. 1973, *A.J.*, **78**, 959.
Liebert, J., Schmidt, G. D., Green, R. F., Stockman, H. S., and McGraw, J. T. 1983, *Ap. J.*, **264**, 262.
Malina, R. F., Bowyer, S., and Basri, G. 1982, *Ap. J.*, **262**, 717.
Margon, B., Liebert, J., Gatewood, G., Lampton, M., Spinrad, H., and Bowyer, S. 1976, *Ap. J.*, **209**, 525.
McCook, G. P., and Sion, E. M. 1984, *Villanova Observatory Contributions*, No. 3.
Moffett, T. J., Barnes, T. G., and Evans, D. S. 1978, *A.J.*, **83**, 820.
Nelan, E. P., and Wegner, G. 1985, *Ap. J. (Letters)*, **289**, L31.
Oke, J. B. 1974, *Ap. J. Suppl.*, **27**, 21.
Petre, R., Shipman, H. L., and Canizares, C. R. 1986, *Ap. J.*, **304**, 356.
Rodgers, A. W. 1971, *Ap. J.*, **165**, 581.
Routly, P. M. 1972, *Pub. U. S. Naval Obs.*, **20**, No. 6.
Sanduleak, N., and Philip, A. G. D. 1968, *Pub. A.S.P.*, **80**, 437.
Schwartz, R. D. 1972, *Pub. A.S.P.*, **84**, 28.
Sonneborn, G., and Garhart, M. P. 1983, *IUE Newsletter*, No. 23, p. 23.
Stewart, J. C., Peek, J. M., and Cooper, J. 1973, *Ap. J.*, **179**, 983.
Tüg, H., White, N. M., and Lockwood, G. W. 1977, *Astr. Ap.*, **61**, 679.
Vidal, C. R., Cooper, J., and Smith, E. W. 1973, *Ap. J. Suppl.*, **25**, 37.
Wegner, G. 1973, *M.N.R.A.S.*, **163**, 381.
———. 1979, *A.J.*, **84**, 1384.
———. 1980, *A.J.*, **85**, 1255.
———. 1983, *A.J.*, **88**, 109.
———. 1984, *A.J.*, **89**, 1050.
Wegner, G., and Schulz, H. 1981, *Astr. Ap. Suppl.*, **43**, 1981.
Wesemael, F., Auer, L. H., Van Horn, H. M., and Savedoff, M. P. 1980, *Ap. J. Suppl.*, **43**, 159.
Wesemael, F., Henry, R. B. C., and Shipman, H. L. 1984, *Ap. J.*, **287**, 868.
Wesemael, F., Liebert, J., and Green, R. F. 1984, *Pub. A.S.P.*, **96**, 981.
Wesselius, P. R., and Koester, D. 1978, *Astr. Ap.*, **70**, 745.
Winget, D. E., Lamb, D. Q., and Van Horn, H. M. 1986, in preparation.

J. BASILE and J. B. HOLBERG: Lunar and Planetary Laboratory, University of Arizona, 3625 East Ajo Way, Tucson, AZ 85713

F. WESEMAEL: Département de Physique, Université de Montréal, C.P. 6128, Montréal, Quebec H3C, 3J7, Canada